Noune, M. B., & Nix, A. R. (2010). Joint Tomlinson-Harashima precoding and optimum transmit power allocation for SC-FDMA. In IEEE Wireless Communications and Networking Conference (WCNC) 2010, Sydney, Australia. (pp. 1 - 6). Institute of Electrical and Electronics Engineers (IEEE). 10.1109/WCNC.2010.5506433

This full text paper was peer reviewed at the direction of IEEE Communications Society subject matter experts for publication in the WCNC 2010 proceedings.

Joint Tomlinson-Harashima Precoding and Optimum Transmit Power Allocation for SC-FDMA

Mohamed Noune and Andrew Nix
Centre for Communications Research, University of Bristol
Merchants Ventures Building, Woodland Road, BS8 1TJ, Bristol UK
Email: {Mohamed.Noune,Andy.Nix}@bristol.ac.uk

***Abstract*— Single-Carrier Frequency Division Multiple Access (SC-FDMA) has been selected as the uplink transmission scheme in the 3GPP Long Term Evolution standard. SC-FDMA has reduced sensitivity to phase noise and a lower Peak-to-Average Power Ratio (PAPR) compared to Orthogonal Frequency Division Multiple Access. In this paper we propose joint Tomlinson-Harashima Precoding and transmit power allocation for SC-FDMA. We derive the optimum power allocation for SC-FDMA transmission for both Zero-Forcing (ZF) and Minimum Mean-Square Error (MMSE) LE receivers in order to maximize the achievable data rate subject to constant transmit power. Although this improves the system's performance and offers a 1-2 dB improvement over Frequency-Domain Decision Feedback Equalization (FD-DFE), when the proposed transmit power allocation scheme is combined with decision feedback equalization the system incurs a performance degradation due to error propagation. In this paper we propose a joint implementation of the derived power allocation scheme with THP. Here we show that the system's performance is further improved over both FD-LE and FD-DFE when transmit power allocation is applied.**

***Index Terms*: 3GPP LTE, SC-FDMA, Waterfilling, Equalization, Precoding, THP.**

I. Introduction

GIVEN its inherent single carrier structure, SC-FDMA has been proposed as the uplink transmission scheme in the 3GPP LTE standard [1]. SC-FDMA can be viewed as DFT precoded OFDMA, and thus has a lower PAPR compared to OFDMA. This makes it more suitable for hand-held devices. SC-FDMA can also be viewed as an Single-Carrier Frequency Domain Equalization (SC-FDE) system with a flexibility in its resource allocation. SC-FDMA can be used with a range of SC-FDE techniques to combat the frequency selective nature of the transmission channel. These include frequency-domain Linear Equalization (LE), Decision Feedback Equalization (DFE) [2], and more recently Turbo Equalization [3]. Frequency-domain LE is analogous to time-domain LE [4], [5]. A Zero-Forcing (ZF) based LE eliminates the ISI completely but degrades the system performance due to noise enhancement. Superior performance can be achieved using the Minimum Mean Square Error (MMSE) criterion. Further improvement can be obtained when the Channel State Information (CSI) is known at the transmitter through dynamic transmit power allocation [7]. A key assumption in the derivation of frequency-domain waterfilling is the use of an optimal receiver. However, when a suboptimal receiver is used, such as the ZF or MMSE frequency-domain linear equalizer, the waterfilling spectrum must be suitably modified [8]. In [9], we have shown that the transmit power allocation scheme in [8], initially proposed for SC-FDE, can be extended to SC-FDMA, in order to exploit the sub-channelization gain in SC-FDMA. As a result, the system can generate multi-user diversity through channel dependent scheduling, or generate a frequency diversity gain through frequency hopping.

To improve the performance of FD-LE, a hybrid time-frequency domain DFE was proposed in [4]. These equalizers are required to produce instantaneous decisions. When incorrect decisions are made, DFEs behave poorly due to error propagation [6], particularly for coded modulation.

In order to overcome these shortcomings we propose the use of Tomlinson-Harashima Precoding (THP) [10]- [11]. THP is an effective way to account for the error propagation problem in a DFE since its feedback filter is implemented at the transmitter and is thus error free [10], [11]. Since precoding does not suffer from error propagation, it can be combined with coded modulation schemes, such as precoding for noise whitening on ISI channels [12] and precoding for partial-channel response [13]. THP, which was originally proposed to combat intersymbol interference for single user transmissions, was shown to be a sub-optimal implementation of Dirty Paper Coding (DPC) [14], and to achieve transmission at the full channel capacity [15]. The dynamic range of the precoded waveform increases in the presence of deep fades in the channel spectrum. To overcome this problem THP is implemented with a modulo operator. Since the operation of THP is tightly connected to the modulated signal constellation, the implementation of THP in the context of SC-FDMA is difficult since the SC-FDMA signal does not have a distinct constellation in the time-domain as a result of oversampling.

This paper is organized as follows. Section II presents the SC-FDMA transmission model. Section III derives the optimum power allocation scheme for FD-LE, and the derivation of the power allocation is performed for both the Zero-Forcing (ZF) and Minimum Mean Square Error (MMSE) criterion. Section IV proposes a modification to the THP coefficients when power allocation is employed. Conclusions are presented in section VI.

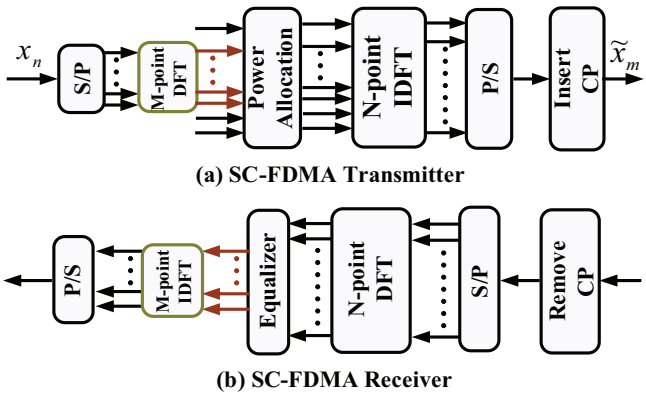

Fig. 1. Proposed SC-FDMA Transmitter Structure with Power Allocation and Frequency Domain Equalization

978-1-4244-6398-5/10/$26.00 ©2010 IEEE

II. Single-Carrier FDMA

Fig. 1 shows the transmitter and receiver structure for an SC-FDMA system with Frequency-Domain optimum power allocation and Frequency Domain Equalization (FDE). For each block of M data samples, $\mathbf{x}$, the transmitter maps the corresponding M frequency components of the block, $\mathbf{X}$, resulting from an $M-$point DFT of the data samples, onto a set of M active sub-carriers selected from a total of $N = QM$ sub-carriers. Here we consider localized and distributed SC-FDMA (L-FDMA and D-FDMA, respectively) [1].

The transmitter performs power allocation prior to sub-carrier mapping by allocating each sub-carrier k with power P_k subject to a limited power constraint. We denote the result of the power allocation mathematically by $\mathbf{PX}$, where the diagonal power allocation matrix $\mathbf{P}$ is given by $\mathbf{P} = diag\{P_0, P_1, \cdots, P_{N-1}\}$.

We define the $N \times M$ sub-carrier mapping transform matrix by $\mathbf{D}$ whose entries are

$$[\mathbf{D}]_{n,m} = \begin{cases} 1 & n = \mathcal{D}(m) \\ 0 & \text{elsewhere,} \end{cases} \tag{1}$$

where the sub-carrier mapping $\mathcal{D}(k)$ for D-FDMA and L-FDMA, [1], are given by equations (2) and (3), respectively

$$\mathcal{D}(k) = s + Q'k \tag{2}$$

$$\mathcal{D}(k) = s + k, \tag{3}$$

where s and Q' denote the sub-carrier of the start of the user's selected sub-channel and the sub-carrier spacing for D-FDMA. Since the columns in both mapping matrices are orthogonal, the de-mapping matrix is $\mathbf{D}^{\mathcal{T}}$. In addition, the mapping matrices $\mathbf{D}_i$ and $\mathbf{D}_j$, for users i and j respectively, must satisfy

$$\mathbf{D}_j^{\mathcal{T}}\mathbf{D}_i = \begin{cases} \mathbf{I}_M & j = i \\ \mathbf{0}_{M\times M} & j \neq i. \end{cases} \tag{4}$$

The sub-carrier mapping produces $\widetilde{\mathbf{X}} = \mathbf{DPX}$. $\widetilde{\mathbf{X}}$ is processed by the N-point Inverse DFT (IDFT) to produce the time-domain transmitted signal $\widetilde{\mathbf{x}}$.

Prior to transmission a cyclic prefix (CP) of length P is inserted into each transmitted block. Although this is performed at the expense of transmission bandwidth, the CP prevents interference from previously transmitted blocks due to multipath delay spread, and hence maintains orthogonality between the sub-carriers. The SC-FDMA transmitted signal is given by

$$\widetilde{\mathbf{x}} = \mathbf{CF}_N^{-1}\mathbf{DPF}_M\mathbf{x}, \tag{5}$$

where $\mathbf{D}$ is the sub-carrier allocation matrix. $\mathbf{F}_N^{-1}$ and $\mathbf{F}_M$ represent the N-point IDFT and M-point DFT matrix respectively. The generic K-point DFT matrix has entries $[\mathbf{F}_K]_{p,q} = 1/\sqrt{K}e^{-\jmath 2\pi\frac{pq}{K}}$, and its inverse is $\mathbf{F}_K^{-1} = \mathbf{F}_K^{\mathcal{H}}$, where $(\bullet)^{\mathcal{H}}$ denotes the *Hermitian* transpose. $\mathbf{C}$ represents the CP insertion matrix,

$$\mathbf{C} = [\mathbf{CP}; \mathbf{I}_N]^{\mathcal{T}}, \quad \mathbf{CP} = \left[\mathbf{0}_{P\times(N-P)}, \mathbf{I}_P\right]^{\mathcal{T}}.$$

After removing the CP at the receiver, the received signal $\mathbf{y} = [y_0, y_1, \cdots, y_{N-1}]$ can be described as

$$\mathbf{y} = \mathbf{H}\widetilde{\mathbf{x}} + \boldsymbol{\eta} = \mathbf{F}_N^{-1}\boldsymbol{H}\mathbf{F}_N\widetilde{\mathbf{x}} + \boldsymbol{\eta}, \tag{6}$$

where $\mathbf{H}$ is a circulant channel matrix, $\boldsymbol{\eta}$ is a column vector containing complex AWGN noise samples, and $\boldsymbol{H}$ is a diagonal matrix, whose entries H_k are generated from the N-point DFT of the channel impulse response.

III. Optimum Power Allocation for FD-LE

This section derives the optimum transmit power allocation matrix $\mathbf{P}$ such that the information rate at the output of the FD-LE is maximized subject to constant transmit power. The optimum transmit power allocation for information rate maximization in single-carrier systems is equivalent to the optimal power allocation for MSE minimization since the SNR at the output of the receiver is a convex function of the MSE and thus minimizing the MSE maximizes the SNR.

For an ISI channel with a channel transfer function H_k, the maximum achievable data rate subject to an input power constraint P is the solution to the following optimization problem

$$\arg\max_{\mathbf{P}} \sum_{k=0}^{N-1} \log_2\left(1 + \frac{|H_k|^2\,|P_k|^2}{\sigma_\eta^2}\right). \tag{7}$$

The constraint on the transmit power is related to the values of the coefficients P_k and can be expressed as

$$\mathrm{tr}\left\{\mathbf{PP}^{\mathcal{H}}\right\} = \sum_{k=0}^{M-1} P_k^2 = \sum_{k=0}^{M-1} \mathcal{P}_k = M, \tag{8}$$

such that $\mathcal{P}_k > 0 : \forall 0 \leq k < M$.

In order to maximize the SNR for ZF FD-LE, we need to minimize the power of the filtered noise at the output of the ZF DF-LE

$$\arg\min_{\mathbf{P}} \quad \sum_{k=0}^{M-1} \frac{1}{\mathcal{P}_k\mathcal{H}_k} \qquad s.t. \qquad \sum_{k=0}^{M-1} \mathcal{P}_k = M, \tag{9}$$

where $\mathcal{H}_k = |H_k|^2$.

This problem can be solved by the use of a *Lagrange* multiplier. The *Lagrange* cost function is given by

$$\mathcal{J}_{\text{ZF}} = \sum_{k=0}^{M-1} \frac{1}{\mathcal{P}_k\mathcal{H}_k} + \lambda\left(M - \sum_{k=0}^{M-1} \mathcal{P}_k\right), \tag{10}$$

where λ is the *Lagrange* multiplier. The optimum solution is obtained by setting the derivative of $\mathcal{J}_{\text{ZF}}$, with respect to $\mathcal{P}_k$, to zero. This is given by

$$\frac{\partial\mathcal{J}_{\text{ZF}}}{\partial\mathcal{P}_k} = -\frac{1}{\mathcal{P}_k^2\mathcal{H}_k} - \lambda, \tag{11}$$

which leads to

$$\frac{\partial\mathcal{J}_{\text{ZF}}}{\partial\mathcal{P}_k} = 0 \Rightarrow \mathcal{P}_k = -\frac{1}{\sqrt{\lambda}}\frac{1}{\sqrt{\mathcal{H}_k}}. \tag{12}$$

Under the total power constraint in equation (9) we can write

$$\sum_{k=0}^{M-1} \mathcal{P}_k = M \Rightarrow -\frac{1}{\sqrt{\lambda}} = \left(\frac{1}{M}\sum_{l=0}^{M-1}\frac{1}{\sqrt{\mathcal{H}_l}}\right)^{-1}. \tag{13}$$

The optimum weights can therefore be found as

$$\mathcal{P}_k = \left(\frac{1}{M}\sum_{l=0}^{M-1}\frac{1}{\sqrt{\mathcal{H}_l}}\right)^{-1}\frac{1}{\sqrt{\mathcal{H}_k}}. \tag{14}$$

The optimum power loading for a ZF FDE-LE is equivalent to a power constrained ZF pre-equalizer, which corresponds to

the optimum power allocation scheme for high SNR regimes. The decision SNR for the ZF receiver, ρ_{ZF}, is given by

$$\rho_{\text{ZF}} = \left(\frac{1}{M} \sum_{k=0}^{M-1} \sqrt{\frac{\sigma_\eta^2}{\sigma_s^2 \mathcal{H}_k}} \right)^{-2}. \quad (15)$$

We can obtain the achievable capacity per unit bandwidth, measured in $bits/sec/Hz$, for the ZF receiver scheme by

$$C_{\text{ZF}} = \log_2 \left[1 + \left(\frac{1}{M} \sum_{k=0}^{M-1} \sqrt{\frac{\sigma_\eta^2}{\sigma_s^2 \mathcal{H}_k}} \right)^{-2} \right]. \quad (16)$$

According to [8], the optimization of the power coefficients for MMSE SC-FDE corresponds to the maximization of the ratio of the desired signal power to the power of the estimated symbol and the filtered noise, which translate to a maximization of the Signal to Interference plus Noise Ratio (SINR). The optimum power allocation condition for the MMSE FD-LE is therefore

$$\arg \max_{\mathbf{P}} \rho_{\text{MMSE}} \qquad s.t. \sum_{k=0}^{M-1} \mathcal{P}_k = M. \quad (17)$$

ρ_{MMSE} is expressed as

$$\rho_{\text{MMSE}} = \frac{M}{\left(\sum_{k=0}^{M-1} \frac{\sigma_\eta^2}{\sigma_s^2 \mathcal{P}_k \mathcal{H}_k + \sigma_\eta^2} \right)} - 1. \quad (18)$$

In order to maximize ρ_{MMSE} we only have to minimize the inverse of $\rho_{\text{MMSE}} + 1$. We define the following *Lagrange* cost function

$$\mathcal{J}_{\text{MMSE}} = \sum_{k=0}^{M-1} \frac{\sigma_\eta^2}{\sigma_s^2 \mathcal{P}_k \mathcal{H}_k + \sigma_\eta^2} + \lambda \left(M - \sum_{k=0}^{M-1} \mathcal{P}_k \right), \quad (19)$$

where λ is the *Lagrange* multiplier. By taking the derivative of $\mathcal{J}_{\text{MMSE}}$ with respect to $\mathcal{P}_k$ we obtain

$$\frac{\partial \mathcal{J}_{\text{MMSE}}}{\partial \mathcal{P}_k} = -\frac{\sigma_s^2 \sigma_\eta^2 \mathcal{H}_k}{\left(\sigma_s^2 \mathcal{P}_k \mathcal{H}_k + \sigma_\eta^2 \right)^2} - \lambda. \quad (20)$$

After rearranging equation (20), the optimum power allocation is given by

$$\frac{\partial \mathcal{J}_{\text{MMSE}}}{\partial \mathcal{P}_k} = 0 \Rightarrow \mathcal{P}_k = \frac{1}{\sqrt{\lambda}} \sqrt{\frac{\sigma_\eta^2}{\sigma_s^2 \mathcal{H}_k}} - \frac{\sigma_\eta^2}{\sigma_s^2} \frac{1}{\mathcal{H}_k}. \quad (21)$$

Under the total power constraint in equation (9), the optimum weights can be found as

$$\mathcal{P}_k = \left[\left(\frac{M + \sum_{l=0}^{M-1} \left(\frac{\sigma_\eta^2}{\sigma_s^2} \frac{1}{\mathcal{H}_l} \right)}{\sum_{l=0}^{M-1} \frac{1}{\sqrt{\mathcal{H}_l}}} \right) \frac{1}{\sqrt{\mathcal{H}_k}} - \frac{\sigma_\eta^2}{\sigma_s^2} \frac{1}{\mathcal{H}_k} \right]^+, \quad (22)$$

where $[\bullet]^+ = \max(\bullet, 0)$. As can be seen, when $\sigma_\eta^2 \longrightarrow 0$, the optimum power allocation scheme for MMSE FD-LE converges towards the optimum power allocation scheme for ZF FD-LE.

IV. Tomlinson-Harashima Precoding

We now consider the Tomlinson-Harashima precoder combined with single-carrier Frequency-Domain Equalization (SC-FDE) for uplink SC-FDMA. We denote this scheme as THP-FDE. The structure of the THP-FDE is shown in Fig. 2 together with its frequency-domain equivalent structure. The operation of the TH-Precoder is described in [10]- [11]. The THP-FDE consists of an L-order feedback filter, $\mathbf{B}(z^{-1})$, a modulo operator at the transmitter and an N tap frequency-domain equalizer at the receiver with weights G_k. The modulo device aims to reduce the dynamic range of the precoded waveform, especially for channels experiencing deep spectral fades. The transfer function of the THP, $\mathbf{B}(z^{-1})$, is given by $\mathbf{B}(z^{-1}) = \sum_{n=1}^{L} b_n z^{-n}$, where b_n are the precoder's coefficients.

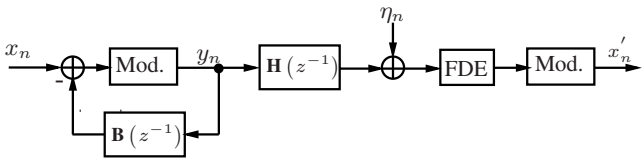

(a) Tomlinson-Harashima Precoding with Frequency-Domain Equalization

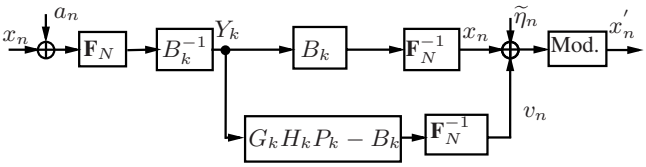

(b) Equivalent Frequency-Domain Structure

Fig. 2. Tomlinson-Harashima Precoding with Frequency-Domain Linear Equalizer and its Equivalent Structure

As a result of precoding the dynamic range of the precoded waveform increases, especially for channels experiencing deep fades. This increases the PAPR of the transmitted waveform. In order to overcome this limitation the THP is implemented with a modulo device. The modulo operation aims to reduce the dynamic range of the precoded waveform, regardless of the precoder's coefficients. For an $\mathcal{M}^2$-QAM constellation, the output of the modulo operation is

$$y_n = x_n - 2\mathcal{M} \left\lfloor \frac{\Re(x_n)}{2\mathcal{M}} + \frac{1}{2} \right\rfloor - j2\mathcal{M} \left\lfloor \frac{\Im(x_n)}{2\mathcal{M}} + \frac{1}{2} \right\rfloor \quad (23)$$

where $\Re(\bullet)$ and $\Im(\bullet)$ denote the real and imaginary parts respectively. $\lfloor \bullet \rfloor$ denotes the flooring operation. x_n, the input of the modulo device, as shown in Fig. 2, is related to the precoder's output by

$$y_n = x_n - \sum_{m=1}^{L} b_m y_{n-m}, \quad (24)$$

where the $\mathcal{M}^2$-QAM symbol x_n is the precoder's input. If we re-arrange both sides of equation (24) and take the N-point DFT of both sides of this equation we obtain

$$X_k = \left(1 + \sum_{n=1}^{L} b_n e^{-j2\pi \frac{kn}{N}} \right) Y_k = B_k Y_k, \quad (25)$$

where B_k denotes the frequency response of the THP filter as shown below

$$B_k = \frac{1}{\sqrt{N}} \left(1 - \sum_{n=1}^{L} b_n e^{-j2\pi \frac{kn}{N}} \right). \quad (26)$$

From [2], the coefficients of the FDE satisfy

$$G_k = \frac{\sigma_s^2 P_k H_k^* B_k}{\sigma_s^2 |P_k H_k|^2 + \nu \sigma_\eta^2}. \quad (27)$$

The output of the FDE is composed of the filtered noise $\widetilde{\eta}_n$ from the FDE, and the residual interference as a result of the precoder. The cost function of the THP-FDE is

$$\mathcal{J}_{\text{THP-FDE}} = \frac{\sigma_\eta^2}{N} \sum_{k=0}^{N-1} \frac{\sigma_s^2 |P_k|^2 |B_k|^2}{\sigma_s^2 |P_k H_k|^2 + \nu \sigma_\eta^2}, \quad (28)$$

where $\nu = 0$ for the ZF THP-FDE and $\nu = 1$ for the MMSE THP-FDE.
We define

$$\phi_n = \frac{1}{\sqrt{N}} \sum_{k=0}^{N-1} \frac{e^{-j2\pi \frac{km}{N}}}{\sigma_s^2 |P_k H_k|^2 + \nu \sigma_\eta^2}, \quad 0 \le n \le L \quad (29)$$

We define the $L \times L$ matrix $\boldsymbol{\varphi}$ and the $L \times 1$ vector $\boldsymbol{\phi}$, such that for all $1 \le l, m \le L$ $[\boldsymbol{\varphi}]_{m,l} = \phi_{l-m}$, and $[\boldsymbol{\phi}]_m = \phi_m$. We define also $\mathbf{b} = [b_1, b_2, \cdots, b_L]$. The mean-square error at the output of the FDE can be expressed as

$$\mathcal{J}_{\text{THP-FDE}} = \phi_0 + \mathbf{b}^{\mathcal{H}} \boldsymbol{\phi} + \mathbf{b}^{\mathcal{H}} \boldsymbol{\varphi} \mathbf{b} + \boldsymbol{\phi}^{\mathcal{H}} \mathbf{b}. \quad (30)$$

The time-domain THP filter coefficients are therefore found by equating the derivative of $\mathcal{J}_{\text{THP-FDE}}$ with respect to $\mathbf{b}^{\mathcal{H}}$ to zero, i.e.,

$$\frac{\partial \mathcal{J}_{\text{THP-FDE}}}{\partial \mathbf{b}^{\mathcal{H}}} = 0 \Rightarrow \boldsymbol{\varphi} \mathbf{b} + \boldsymbol{\phi} = 0 \quad \Rightarrow \boldsymbol{\varphi} \mathbf{b} = -\boldsymbol{\phi}. \quad (31)$$

Since the operation of THP is tightly connected to the signal constellation, the implementation of THP in the context of SC-FDMA becomes difficult since the SC-FDMA time-domain waveform does not have a distinct constellation. In [16], we have proposed a frequency-domain implementation of the THP filter by removing the modulo device and converting the time-domain cyclical convolution between the transmitted signal and the THP filter into a point–by–point multiplication in the frequency-domain; If the precoder's input is the SC-FDMA modulated signal, $\widetilde{\mathbf{x}}$ after CP insertion, then by ignoring the first P samples the precoder's output $\mathbf{y}_n$ can be related to the precoder's input $\mathbf{x}$, expressed as $\mathbf{y} = \mathbf{B}\widetilde{\mathbf{x}}$, where $\mathbf{B}$ is a circulant matrix. The precoder's output is therefore

$$\mathbf{y} = \overline{\mathbf{B}}^{-1} \widetilde{\mathbf{x}} = \mathbf{F}_N^{-1} \boldsymbol{\Pi} \mathbf{D} \boldsymbol{\Pi} \mathbf{D} \mathbf{P} \mathbf{F}_M \mathbf{x}, \quad (32)$$

where $\boldsymbol{\Pi}$ is a diagonal matrix with entries B_k^{-1}, where B_k is given in equation (26).
We denote by Ψ_i the sub-carrier occupied by user i. We define the impulse response $\widetilde{\mathbf{B}}\left(z^{-1}\right) = \sum_{n=1}^{L_b} \widetilde{b}_n z^{-n}$, such that

$$\widetilde{b}_n = \frac{1}{\sqrt{M}} \sum_{k \in \Psi_i} B_k e^{j2\pi \frac{kn}{M}}. \quad (33)$$

We refer to this scheme as pre-DFT THP since the THP filter [17], which consists of an L_b-order feedback filter, as it is applied to the input of the M-point DFT in the SC-FDMA transmitter. It should be noted that the pre-DFT THP yields the same performance as the FD-THP [17]. When combined with a modulo operator, the pre-DFT time-domain THP precoder results in reduced dynamic range compared to the frequency-domain implementation, which results in a lower PAPR in the transmitted signal. Despite this reduction in PAPR, as a result of spectral leakage, the order of the pre-DFT THP precoder becomes $L_b = M$, which leads to increased complexity.

As a result of precoding, the mean transmit power per SCFDMA symbol increases or decreases as a result of the magnitude fluctuations of the precoder's weights. Since the transmit power per symbol is limited, we should maintain the same mean transmit power per symbol as the case with no precoding. Therefore, the weights of the precoder must be power constrained. For each precoded SC-FDMA symbol, the mean transmit power is given by

$$\frac{1}{M} \sum_{k \in \Psi_i} \left| B_k^{-1} P_k \widetilde{X}_k \right|^2 = \frac{\sigma_s^2}{M} \sum_{k \in \Psi_i} \left| B_k^{-1} P_k \right|^2 = \gamma^2 \sigma_s^2 \quad (34)$$

where γ denotes the gain in the transmit power as a result of precoding and is given by $\gamma = \sqrt{\frac{1}{M} \sum_{k \in \Psi_i} \left| B_k^{-1} P_k \right|^2}$. In order to normalize the transmit power to the case with no precoding, the precoder's output is divided by γ. As a result of power normalization, the output of the FDE from equation becomes

$$\widehat{x}_n = \frac{1}{\gamma} x_n + \frac{1}{\gamma} \frac{1}{M} \sum_{k \in \Psi_i} \left(G_k H_k P_k - B_k \right) Y_k e^{j2\pi \frac{kn}{M}} + \widetilde{\eta}_n. \quad (35)$$

This means that power normalization at the transmitter results in a gain mismatch at the output of the receiver. Since we assume that the transmitter and receiver are perfectly synchronous and that the multipath channel is static and perfectly known at both sides of the link, in order to compensate for the gain mismatch between the transmitter and receiver, the output of the receiver must be multiplied by γ. Therefore, from equation (35)

$$\gamma \widehat{x}_n = x_n + \frac{1}{M} \sum_{k \in \Psi_i} \left(G_k H_k P_k - B_k \right) Y_k e^{j2\pi \frac{kn}{M}} + \gamma \widetilde{\eta}_n \quad (36)$$

Although multiplying the output of the FDE by γ removes the gain mismatch between the transmitter and receiver, it also results in noise enhancement.

V. Results and Discussions

In all the following simulations, a range of QAM constellations are used. We assume that the total number of sub-carriers is $N = 512$. The CP length for each frame is P = 64, and we use 1,000 frames for all SNR values. Performance is averaged over time-invariant frequency-selective fading channels, where the channel remains static during each frame and varies from one frame to another. A 6-tap Typical Urban channel (TU6) is used, such that the fading on each tap is assumed to follow a complex independent and identically distributed (i.i.d.) Rayleigh distribution.

A. FD-LE-WF PAPR Statistics

Figure 3 shows the Complementary Cumulative Density Function (CCDF) of the PAPR of the transmitted SC-FDMA waveform with optimum transmit power allocation based on ZF and MMSE frequency-domain linear equalizers. The PAPR of the optimum transmit loading scheme varies with modulation order and FD-LE algorithm. This is due to the

different gains on each of the sub-carriers, which depend on the channel impulse response. We also observe that the PAPR of 16-QAM is higher than the PAPR of QPSK and both the ZF and MMSE schemes result in a PAPR that is higher than conventional SC-FDMA. Furthermore the PAPR of the MMSE optimum loading scheme is higher than both the ZF and the SC-FDMA waveform.

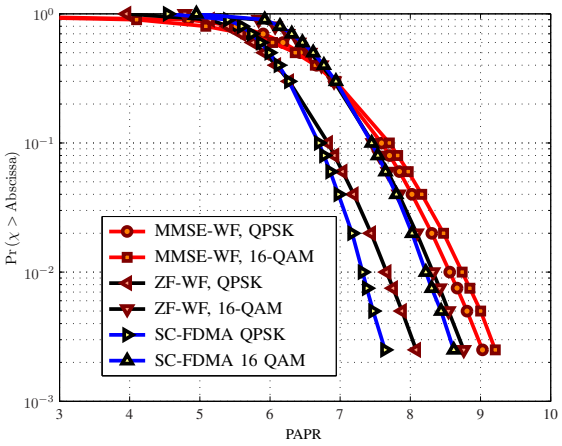

Fig. 3. PAPR of the SC-FDMA waveform with Optimum Transmit filter for ZF and MMSE FD-LE for ($Q = 2$).

Fig. 4 shows the CCDF of the PAPR for the ZF and MMSE THP waveforms for different values of M, calculated for each SC-FDMA symbol. As can be seen, the PAPR of the ZF-THP is higher than the PAPR of the MMSE-THP, for all M. For example, the 99% PAPR level (the PAPR level χ that satisfies Pr(PAPR$>\ \chi$)=0.01) for $Q = 4$ offers an improvement of 1dB compared to $Q = 2$ and an improvement of almost 2dB compared to $Q = 1$ for both ZF and MMSE THP, which in addition to the sub-channelization gain offers a further improvement in the mean transmit power as Q grows larger (smaller M).

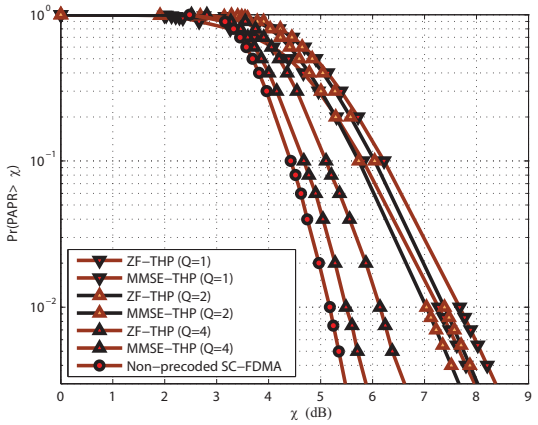

Fig. 4. PAPR Characteristics of the precoded SC-FDMA waveform.

B. Receiver Performance

The BER performance of the optimum waterfilling and the uniform-power distributed system improves, while the performance of the proposed power allocation for FD-LE degrades. This is due to error propagation in both noise-prediction (NP) and decision-feedback equalization (DFE) structures, which degrades the receiver's performance. In addition, the FD-LE

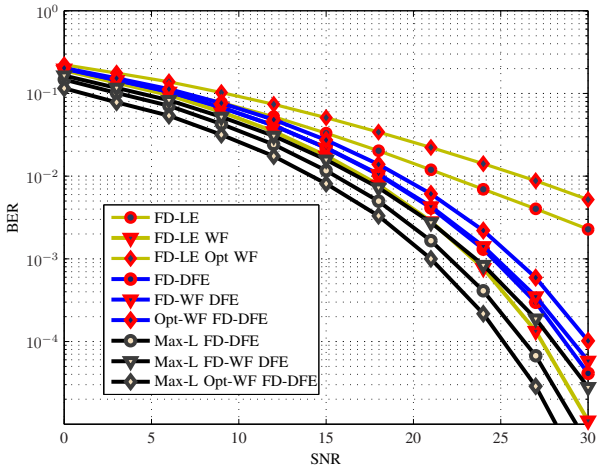

Fig. 5. BER Performance of FD-DFE with Different Power Allocation Schemes for SC-FDE.

with the proposed power allocation offers a 1-2 dB improvement over FD-DFE. For maximum-length noise prediction (an FD-DFE with 511 feedback taps), the optimum waterfilling based transmit filter outperforms both the FD-LE and the proposed power allocation scheme. This indicates that the proposed scheme becomes sub-optimal as the order of the FD-DFE filter increases, while the optimum waterfilling benefits from the improvement offered by the DFE. This is explained as follows. The maximum length FD-DFE cancels the residual ISI at the output of the FD-LE and reduces the variance of the filtered noise. Since it was shown in [7] that the *unbiased* MMSE DFE achieves the same capacity of the underlying channel, the optimum waterfilling transmit filter achieves a better performance than both the proposed transmit power allocation and the uniform-power distributed transmit filter. For this reason, the degree of improvement offered by the optimum waterfilling is greater than that of each of the other two schemes.

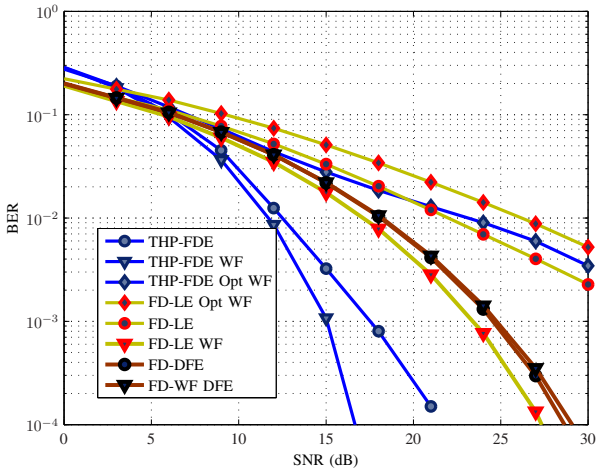

Fig. 6. BER Performance of THP-FDE with Different Power Allocation Schemes for SC-FDE.

Fig. 6 shows the performance of uncoded THP-FDE compared to both FD-LE and FD-DFE, for different transmit filters. The results show that the THP-DFE for the proposed scheme and uniform-distributed transmit power achieve a performance improvement over FD-DFE. In addition, the THP-FDE with the proposed scheme achieves the lowest

BER compared to the other schemes. In addition, comparing figures 6 and 5, the THP-FDE with the proposed scheme improves the performance of the FD-LE with the same power allocation, unlike the FD-DFE. This is because the THP-FDE does not suffer from error propagation.

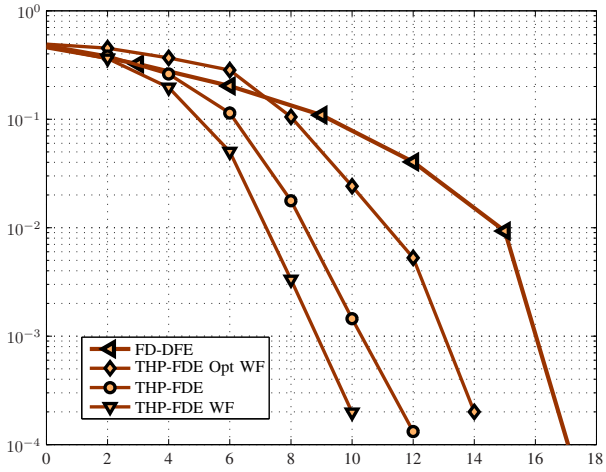

Fig. 7. BER Performance of Coded THP-FDE with Different Power Allocation Schemes for SC-FDE.

Fig. 7 and Fig. 8 show the BER performance for coded QPSK modulation for the proposed power allocation and optimum waterfilling and the throughput of the THP-FDE with different power allocation schemes. The results were generated using a 1/2 rate encoder with octal generator polynomials $[133, 171]_8$, and assuming a hard-decision Viterbi decoder. For the proposed power allocation scheme, it can be seen that the THP-FDE WF offers a better BER performance and achieves higher throughputs compared to the THP with uniform-distributed power and THP with optimum waterfilling.

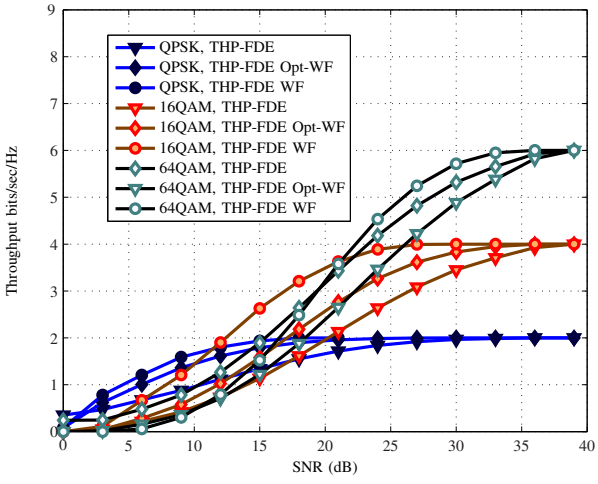

Fig. 8. Throughput of THP-FDE with the Different Power Allocation Schemes.

VI. Conclusion

Frequency-domain linear and decision feedback equalization are two common assumptions in SC-FDMA. The former suffers from a fundamental performance degradation as a result of noise enhancement and residual ISI, while the latter suffers from performance degradation as a result of error propagation, especially for coded modulation. To overcome these problems, in this paper we have presented a novel transmit power allocation scheme for FD-LE and the joint implementation of the power allocation scheme with THP.

The proposed power allocation scheme was seen to outperform FD-LE with uniform-distributed power and optimum waterfilling transmit filters, and also offers an advantage over FD-DFE, yet when combined with FD-DFE, the proposed power allocation does not perform as well as optimum waterfilling, particularly when the length of the feedback filter increases. On the other hand, when combined with THP for uplink SC-FDMA transmission, the overall system performance is further increased.

Acknowledgment

The authors would like to thank the Centre for Communications Research for the provision of research facilities and access to a high performance computing cluster.

References

[1] Hyung G. Myung, “Single Carrier Orthogonal Multiple Access Technique for Broadband Wireless Communication”, Polytechnic University, January 2007

[2] N. Benvenuto and S. Tomasin, “On the Comparison between OFDM and Single-Carrier Modulation with a DFE Using a Frequency-Domain Feedforward Filter,” IEEE Trans. Commun., vol. 50, no. 6, pp. 947-955, Jun. 2002.

[3] G. Berardinelli, B. E. Priyanto, T. B. Sørensen, and P. Mogensen, “Improving SC-FDMA Performance by Turbo Equalization in UTRA LTE Uplink,” IEEE Vehicular Technology Conference (VTC) 2008 Spring, Marina Bay, Singapore, May 2008

[4] David Falconer, S. Lek Ariyavisitakul, Anader Benyamin-Seeyar, Brian Eidson, “Frequency Domain Equalization for Single-Carrier Broadband Wireless Systems”, Communications Magazine, IEEE, Apr. 2002

[5] H. Sari, G. Karam, and I. Jeanclaude, “Transmission techniques for digital terrestrial TV broadcasting,” IEEE Communications Magazine, vol. 33, no. 2, pp. 100109, 1995.

[6] F. Pancaldi, G. M. Vitetta, R. Kalbasi, N. Al-Dhahir, M. Uysal and H. Mheidat, “Single-Carrier Frequency Domain Equalization,” IEEE Signal Process. Mag., vol. 5, no. 12, pp. 3548-3557, Sep. 2008

[7] R. F. Fischer, “Precoding and Signal Shaping for Digital Transmission,” John Wiley & Sons, 2002

[8] D.Z. Filho, L. Féty, and M. Terré, “A hybrid single-carrier/ multicarrier transmission scheme with power allocation,” EURASIP J. Wirel. Commun. Netw., vol. 2008, no. 1, pp. 1–8.

[9] M. Noune, A. Nix, “Optimum Transmit Filter for Single-Carrier FDMA with Frequency-Domain Linear Equalization,” Accepted for participation in IEEE PIMRC 2009, Japan, Sep. 2009.

[10] M. Tomlinson, “New automatic equalizer employing modulo arithmetic,” Electron. Lett., vol. 7, pp. 138-139, Mar. 1971.

[11] H. Harashima and H. Miyakawa, “Matched-transmission technique for channels with intersymbol interference,” IEEE Trans. Commun., vol. 20, pp. 774-780, Aug. 1972.

[12] R. Laroia, S. Tretter and N. Farvardin, “A Simple and Effective Precoding Scheme for Noise Whitening on Intersymbol Interference Channels”, IEEE Trans. on Communications, October 1993.

[13] Lee-Fang Wei, “Precoding Technique for Partial-Response Channels with Applications to HDTV Transmission”, IEEE Journal on Selected Areas in Communications 11(1): 127-135 (1993)

[14] C. B. Peel, “On “dirty-paper-coding”,” IEEE Signal Processing Magazine, vol. 20, no 3, pp 112–113, May 2003

[15] R. D. Wesel, J. M. Cioffi: “Achievable Rates for Tomlinson-Harashima Precoding,” IEEE Transactions on Information Theory, vol. 44, no 2, pp 824-831, 1998

[16] M. Noune and A. Nix, “Frequency-domain precoding for single carrier frequency-division multiple access,” IEEE Comms. Process. Mag., vol. 47, no. 6, pp. 68–74 , Jun. 2009

[17] M. Noune and A. Nix, “Tomlinson-Harashima Precoding for SC-FDMA,” Presented at Eusipco, Glasgow 2009, August 2009